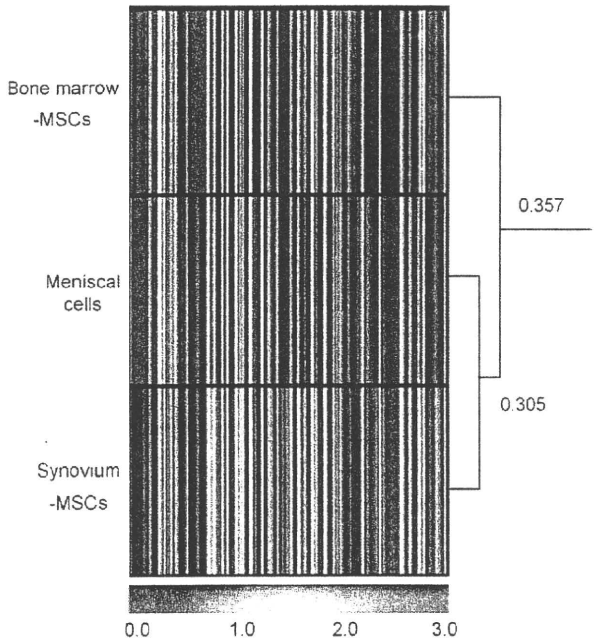

Figure 2. Dendrogram resulting from a hierarchically clustering analysis for gene profile of rat bone marrow-MSCs, synovium-MSCs, and meniscal cells. Gene expression was analyzed with the GeneChip Rat 230 2.0 probe arrays. Data of 14,882 probe sets were analyzed by applying a hierarchical tree algorithm to the normalized intensity. The color code for the signal strength in the classification scheme is shown in the box below. High-expression genes are indicated by shades of red and low expression genes are indicated by shades of blue. The dendrogram at the right provides a measure of the relatedness of gene expression profile in each sample (one minus the Pearson correlation). Abbreviation: MSCs, mesenchymal stem cells.

of the knee of wild rats (Fig. 3A), and Luc/LacZ^{+} synovium-MSCs suspension (5×10^6 in 50 μl PBS) were injected into the right knee joint immediately after the incision was closed. For the control, the same volume of PBS was injected into the left knee. At 2 weeks, dark blue areas for LacZ were observed around the meniscal defect (Fig. 3B, yellow arrow) and sutured capsule (black arrow), indicating that injected synovium-MSCs intensively adhered to injured sites. Dark blue areas for LacZ were still observed around the meniscal defect and sutured capsule, but not observed in intact synovium, cartilage surface, or cruciate ligaments even at 12 weeks (data not shown). At 4 weeks, the anterior part of the meniscal defect of MSC injection side exhibited better regeneration than the control side (Fig. 3C).

All menisci for the experiment of synovium-MSCs are shown in Figure 3D. At 2 weeks, the regenerated part of the menisci appeared blue after X-gal staining in the MSC injection group, indicating that injected synovium-MSCs contributed to the repair. Square measures of the meniscus in synovium-MSCs injection groups were significantly larger than those in the control groups at 2, 4, and 8 weeks (Fig. 3E). We also evaluated cartilage and observed fibrillation, ones of the degenerative changes on the surface of the medial femoral condyle and medial tibial plateau in the control group at 12 weeks (Fig. 3F).

When we injected the same amount of bone marrow-MSCs, the meniscal defect was more rapidly regenerated than that on the control side at 4 weeks (Fig. 3D). Macroscopically, there were no remarkable differences between the synovium-MSC injection group and the bone marrow-MSC injection group.

Histologically, the contour of the regenerated menisci sharpened and the ultimate forms were closer to the normal meniscal shape (Fig. 4A). Expression of type II collagen increased in a time-dependent manner. LacZ^{+} MSCs still existed at 12 weeks. In the control group at 12 weeks, regenerated tissue was occupied with less metachromasia, and type II collagen expression was hardly detected. In the bone marrow-MSC injection group, we observed similar features as seen in the synovium-MSC injection group (Fig. 4B).

Electron microscopic analysis of the regenerated meniscus 12 weeks after synovium-MSCs injection demonstrated that round cells with short processes were surrounded by a pericellular matrix, suggesting that meniscal cells were morphologically equivalent to those of the normal meniscus. In contrast, the cell feature in control groups remained to be fibroblastic (Fig. 4C).

Injected MSCs Stay in Knee Joint

The distribution of topically injected synovium-MSCs was evaluated using luciferase-based in vivo imaging. When MSCs were injected into the normal knee ($n = 4$), MSC-derived photons were detected around the right knee, to then decrease within 14 days. When injected into menisectomized knee ($n = 7$), the photons increased in 3 days, then moderately decreased, but could be still observed for 28 days. Substantial luminescence light could not be detected in any other organs of either group (Fig. 5A). Sequential quantification demonstrated that luciferase activities were significantly higher in the meniscectomy group than those in the control group at each time point up to 21 days (Fig. 5B).

To further evaluate whether injected MSCs could migrate to distant organs or not, quantitative real-time PCR was performed. Total RNAs were isolated from the brain, lung, liver, spleen, kidney, and knee synovium of meniscectomized rat at 3 days after the synovium-MSC injection, and were subjected to *real-time PCR* to measure the level of LacZ expression. Injected MSC-derived LacZ gene could be detected only at the injected knee synovium and was not detected in any other organs (Fig. 6). These data confirm the in vivo imaging results and indicate that knee-injected MSCs stayed only in the knee joint.

Discussion

A number of reports have previously described the injection of bone marrow-MSCs into the joint for meniscus injury; however, the kinetics and role of injected MSCs remain unknown. In a goat study, a previously removed medial meniscus regenerated 6 months after MSC injection [16]. However, Caplan et al. suggested in their review article that there were too few prelabeled cells to account for the massive regeneration of the meniscus and inferred that the MSCs trophically enhanced the regeneration of the meniscus [17]. In two other articles, cartilage matrix was present around injected bone marrow MSCs in only a small portion of the injured meniscus, but the roles of injected MSCs were not fully demonstrated [18, 19] To refine our analysis, we created Tg rats expressing dual Luc/LacZ genes.

There are three main factors involved in the interaction between injected synovium-MSCs and meniscal defect: (a) an increase and decrease in the number of the cells, (b) an adherence to the meniscal defect, and (c) differentiation and maintenance.

In in vivo imaging analysis, synovium-MSCs injected into the menisectomized knee transiently increased in number unlike the situation in which the same population of the cells was injected into the intact knee. This indicates that meniscus injury or incision of the articular capsule can produce some cytokines/chemokines to proliferate synovium-MSCs. In a rabbit model,

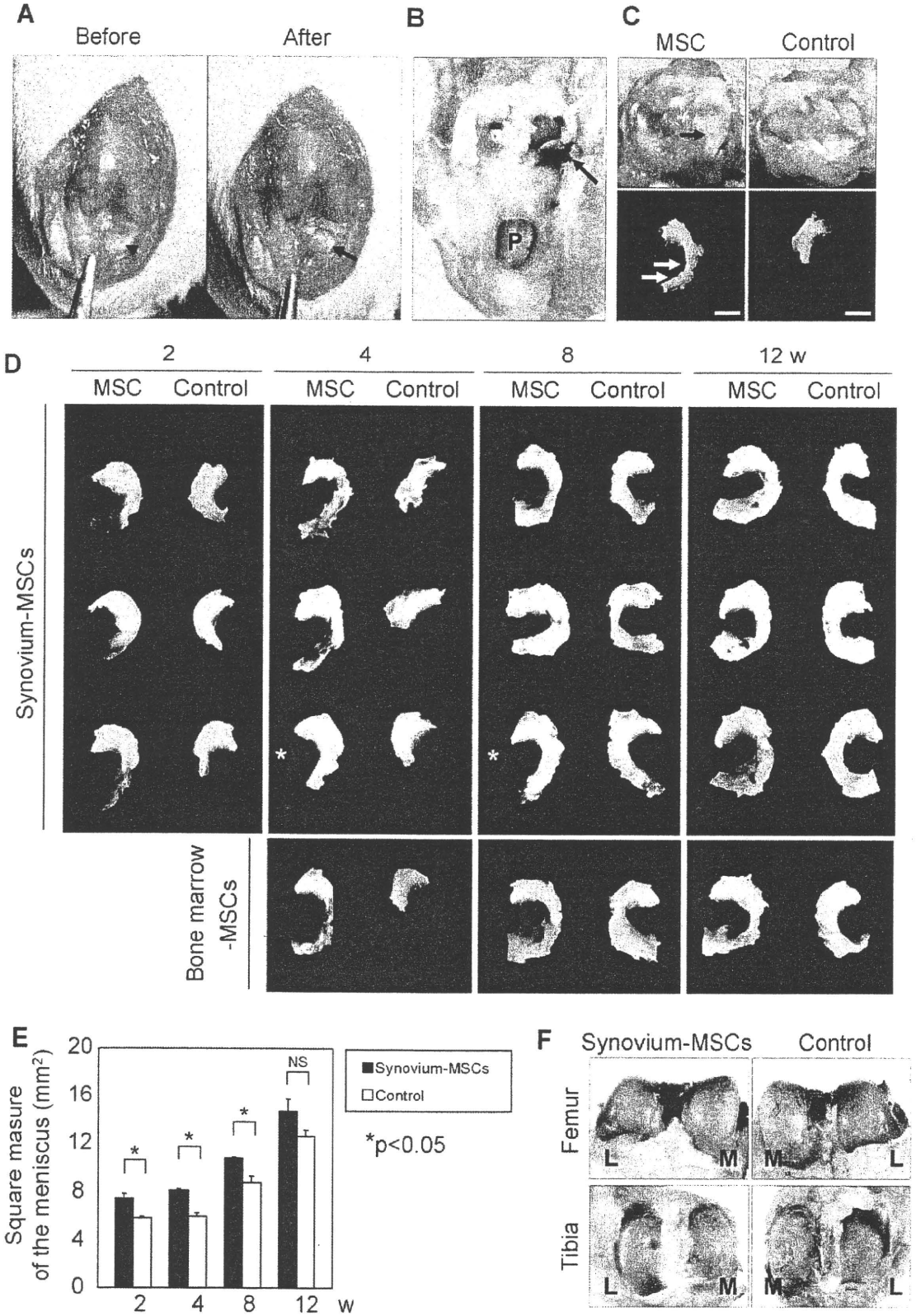

Figure 3. Macroscopic observation of meniscal regeneration after intra-articular injection of synovium-MSCs derived from Luc/LacZ transgenic (Tg) rats. **(A):** Surgical procedure for massive meniscectomy of a wild rat. The medial meniscus was dislocated anteriorly (left, arrowheads), the anterior half of the meniscus was excised, and tibial cartilage was exposed (right, arrow). **(B):** Macroscopic findings of the meniscectomized knee 2 weeks after the injection of synovium MSCs. The knee was stained with X-gal. LacZ positive areas were revealed around the meniscal defect (yellow) and sutured capsule (black). **(C):** Representative macroscopic findings of the tibial joint 4 weeks after synovium-MSCs injection. In the MSC injection group (left), the anterior part of meniscal defect has regenerated (arrow), whereas in the control group, the meniscal defect remains unchanged. Scale bar: 2 mm. **(D):** Macroscopic findings of the regenerated meniscus at 2, 4, 8, and 12 weeks. All menisci were stained with X-gal except those denoted by an asterisk. Representative macroscopic observation of meniscal regeneration after intra-articular injection of bone marrow-MSCs derived from Luc/LacZ Tg rats are shown in the lower part. **(E):** Sequential quantification for area of the meniscus. Values are averages with standard deviations ($n = 3$ for each group). *$p < .05$ between the synovium-MSC group and the control group at each period by Mann-Whitney U test. **(F):** Representative macroscopic findings of the joint surface of femur and tibia 12 weeks after the synovium-MSC group and the control group. The cartilage was stained with India ink. Abbreviations: L, lateral; M, medial; MSCs, mesenchymal stem cells; NS, not significant; P, patella.

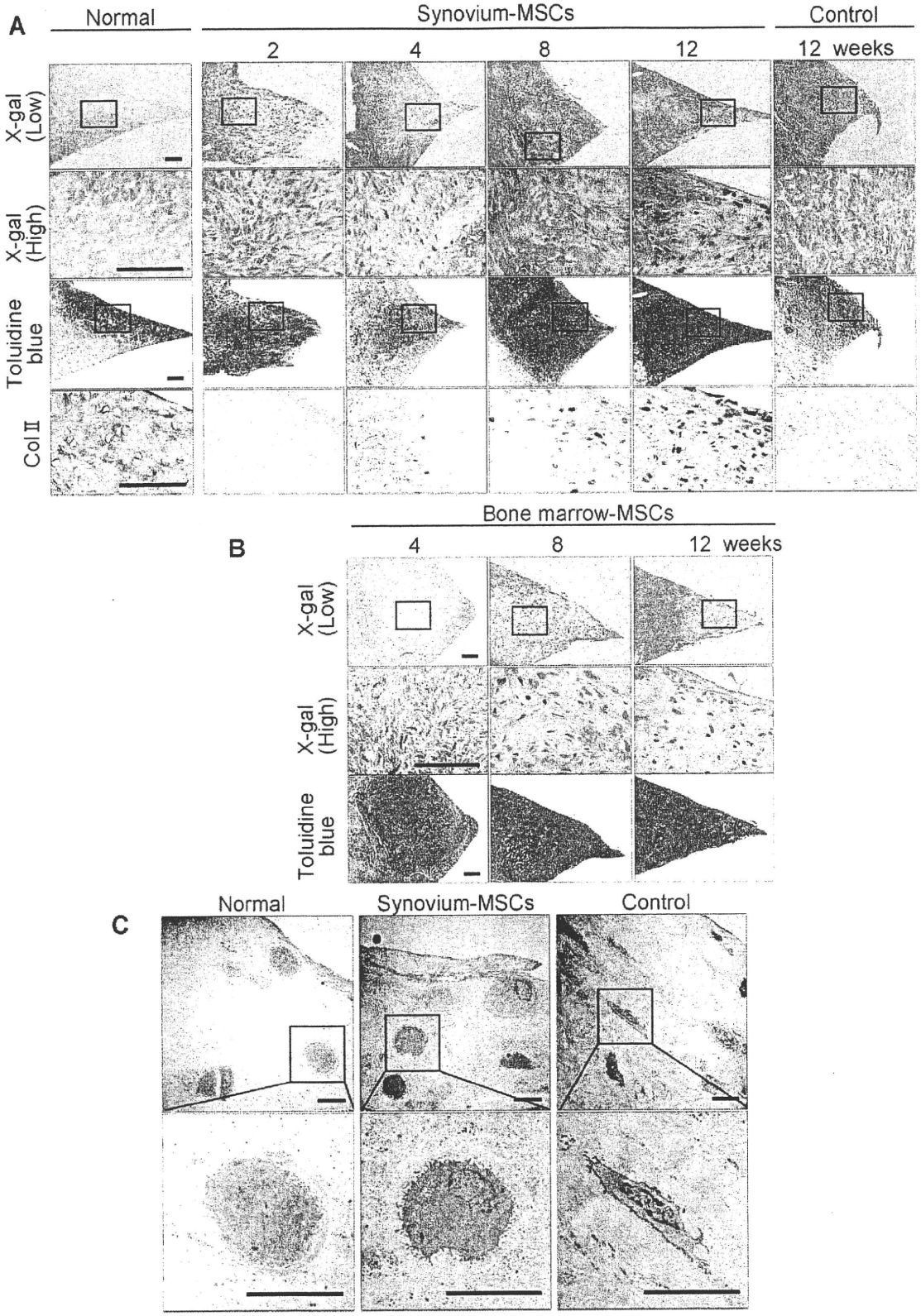

Figure 4. Histological observation of meniscal regeneration after the intra-articular injection of MSCs derived from Luc/LacZ transgenic rats. **(A):** Representative sections of normal meniscus and regenerated tissues in the synovium-MSC injection group stained with X-gal (and eosin as counter staining), toluidine blue, and immunostained with collagen type 2. Scale bar = 100 μm. **(B):** Representative sections of regenerated tissues in the bone marrow-MSC injection group stained with X-gal (and eosin as counter staining), toluidine blue. Scale bar: 100 μm. **(C):** Transmission electron microscopy imaging of typical cells in normal meniscus, regenerated part of meniscus both in the synovium-MSC injection group, and the control group at 12 weeks. Scale bar = 10 μm. Abbreviation: MSCs, mesenchymal stem cells.

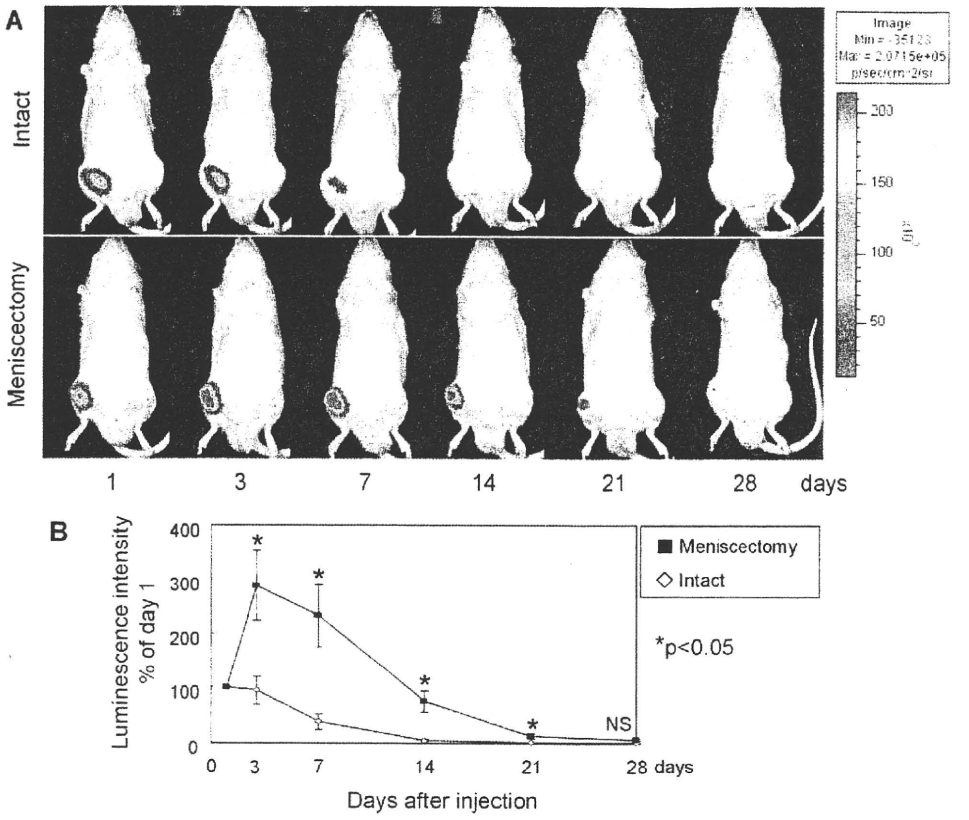

Figure 5. In vivo imaging analysis. **(A):** Imaging of photons from Luc+ cells. Five million synovium-mesenchymal stem cells (MSCs) derived from Luc/LacZ transgenic rats were injected into the intact knee or the meniscectomized knee. Luciferin was injected into the penile vein at indicated points to monitor luminescence driven by synovium-MSCs. **(B):** Sequential quantification of luminescence intensity. Average percentages of the value at 1 day are shown with standard deviations. $*p < .05$ between menisectomy group ($n = 7$) and intact group ($n = 4$) at each period by Mann-Whitney U test. Abbreviations: Max, maximum; Min, minimum; NS, not significant.

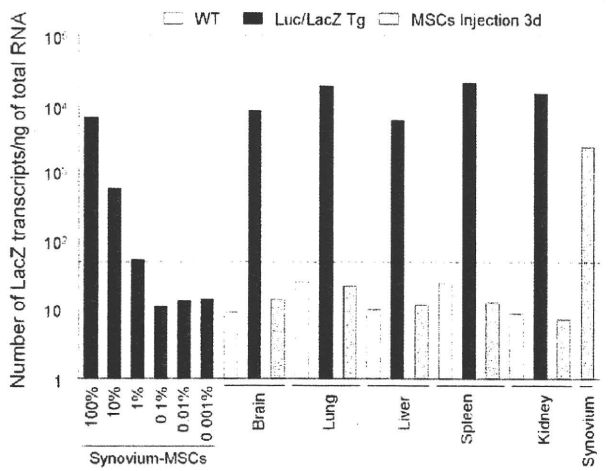

Figure 6. Real-time PCR analysis. The mRNA levels of LacZ obtained from expanded synovium-MSCs and various organs (brain, lung, liver, spleen, kidney, and knee synovium) were determined by SYBR green-based real-time quantitative RT-PCR. The copy number is expressed as the number of transcripts per nanogram of total RNA. The dashed line shows the minimum detection limit (50 copies per nanogram) which was determined by these dilution series. Abbreviations: MSCs, mesenchymal stem cells; Tg, transgenic; WT, wild-type.

meniscal lesions expressed TGF-β, interleukin-1α, and platelet derived growth factor (PDGF) [20]. Human synovium-MSCs have PDGF receptor α and β, and neutralizing PDGF decreases the proliferation of synovium-MSCs in vitro [21]. PDGF may affect the number of transplanted synovium-MSCs.

We could detect MSC-derived photons in the knee joint up to 28 days after the injection but we could not detect it at a longer time point. We have two speculations about this result. One is that a luciferase-based in vivo imaging system cannot detect a small number of Luc^+ cells, as shown in Figure 1D. More than 1,000 cells are needed to detect the light emission. The other is due to blood circulation. The photons are produced only when luciferase is exposed to luciferin substrate and we injected luciferin intravenously. If the Luc^+ cells had existed in the hypovascular area, they could not have been detected. However, in vivo imaging analysis has a great advantage in tracking cells in vivo because we did not have to sacrifice animals, and we could observe the same recipient throughout the observation periods.

Those synovium-MSCs which seem unnecessary for meniscal repair decreased in number and finally fell below measurable limits based on an in vivo imaging system. Possibly, synovium-MSCs participate in intra-articular tissue homoeostasis and repair as do MSCs in mesenchymal tissues throughout the body. This phenomenon differs markedly from ES cells, which form teratomas in the mouse knee joint and subsequently destroy the joint [22]. Induced pluripotent stem cells may hold attraction for future applications, but teratoma formation cannot be overlooked [23].

In vivo imaging analysis suggests that the injected cells did not mobilize out of the injected joint. To confirm this result, we performed real-timePCR to detect Lac Z transcripts. We determined that LacZ transcripts were not detected in brain, lung, liver, spleen, or kidney 3 days after the injection, although the minimum detection limit was 50 copies per nanogram RNA which corresponded to 1% $LacZ^+$ cells. Detection of $LacZ^+$ cells in all sections thorough whole tissues will provide data from another point of view; however, it will be very arduous work.

Injected synovium-MSCs intensively adhered to injured sites of meniscus and synovium. We previously reported that injected synovium-MSCs efficiently adhered to the defect of

articular cartilage [24] and anterior cruciate ligament [6]. The mechanisms that guide the homing of injected cells are not well-understood, but stromal cell-derived factor-1 and monocyte chemotactic protein-1 are candidates to explain them [17].

Undifferentiated synovium-MSCs, attached around the meniscal defect, differentiate into meniscal cells. The environment of the meniscal defect is surrounded by femur and tibia cartilage, synovial tissue, the remaining meniscus, and synovial fluid. The space is also influenced by mechanical stress. This environment itself will provide sufficient signals to induce and maintain meniscal differentiation of synovium-MSCs. Similarly, undifferentiated synovium-MSCs implanted onto an articular cartilage defect differentiate into cartilage cells [25].

In our massive meniscectomized model, bone marrow-MSCs also promoted meniscus regeneration. There were no notable differences of regenerated meniscus in morphology between the synovium-MSC group and the bone marrow-MSC group, although gene profile of synovium-MSCs is closer to that of meniscal cells than that of bone marrow-MSCs. The situation seems to be similar in chondrogenesis as was the case in our previous studies. The gene profile of synovium-MSCs is closer to that of chondrocytes than that of bone marrow-MSCs [26], transplanted bone marrow-MSCs onto the cartilage defect differentiated into chondrocytes at a similar level to that synovium-MSCs which were transplanted in the same way [27]. In contrast, in vivo chondrogenic assay demonstrated that synovium-MSCs produced more cartilage matrix than bone marrow-MSCs [4, 5]. An in vivo model with more sensitivity may distinguish the difference.

Although reparative potential of synovium- and bone marrow-MSCs is similar, synovium-MSCs have an advantage in that they have a higher proliferation potential. In rats, the colony number per nucleated cell was approximately 1/100 in synovium, whereas it was $4/10^5$ in bone marrow. Rat synovium-MSCs expanded much faster than bone marrow-MSCs [5]. Also, human synovium-MSCs proliferated much faster than bone marrow-MSCs when cultured with autologous human serum [21].

For adipogenesis, it usually takes 3 weeks for human bone marrow MSCs to differentiate into adipocytes [10]. In this study, rat bone marrow- and synovium-MSCs differentiated into adipocytes in only 4 days, which was similar to our previous report [5]. Although the content of the adipogenic differentiation medium is similar, the duration to induce sufficient accumulation of lipid vesicles is totally different between MSCs in humans and rats. This indicates the species specificity of MSCs.

For calcification, we found that rat MSCs already calcified in 3 weeks, which was similar to our previous report [5]. In this study, we expected that the calcified area would increase after an additional 3 weeks; therefore, we observed calcification for a total of 6 weeks. Seemingly, the calcified area did not increase during the last 3 weeks (data not shown).

We previously created a 1 mm diameter cylindrical defect in the anterior part of medial meniscus in rats to examine the effect of synovium-MSCs injected intra-articularly. Contrary to our expectation, the cylindrical defect was filled spontaneously, and there was no effect on injected synovium-MSCs through 2-12 weeks [28]. To avoid spontaneous healing, we resected the anterior half of medial meniscus for this study. Meniscal size also increased in the control group, and the difference of meniscal size between the two groups disappeared at 12 weeks; however, the synovium-MSC injected groups showed better results from the standpoint of type II collagen expression and electron microscopic features.

For clinical application, interspecies differences have to be considered. The inherent healing capacity of the meniscus has been shown to be lacking in the inner third and is very limited in the middle third of this poorly vascularized tissue in humans [29] and dogs [30]. We used a rat model, and rat meniscus had a greater spontaneous healing potential. To demonstrate the effectiveness of intra-articular injection of synovium-MSCs for meniscus regeneration, further experimental studies in larger animals are needed.

Native meniscus play an important role in knee stability and shock absorption [31], and this property is linked to the biphasic microstructure of the meniscus [32]. The extracellular matrix of the meniscus is composed mainly of collagen, with smaller quantities of proteoglycans, matrix glycoproteins, and elastin [33]. In this study, we showed that in the synovium-MSC injection group, the menisci regenerated much better than it did in the control group morphologically, and synovium-MSC injection prevented cartilage degeneration at 12 weeks after the meniscectomy as shown in Figure 3F. However, our data lack the details about biomechanical and biochemical properties of regenerated tissues, and it is still uncertain whether the regenerated menisci function in a normal manner and prevent secondary osteoarthritic change in the long term. Therefore, future studies should include biomechanical and biochemical analysis of the regenerated menisci.

Recently, we reported that human synovium-MSCs increased in synovial fluid after intra-articular ligament injury and that exogenous synovium-MSCs adhered to the injured ligament in a rabbit model [6, 34]. We also demonstrated that autologous synovial fluid enhanced migration of MSCs from synovium of osteoarthritis patients in a tissue culture system seemingly to delay the progression of the cartilage degeneration [7]. We speculate that synovial tissue may serve as a reservoir of stem cells that mobilize following intra-articular tissue injury and migrate to the site to participate in the repair response.

According to our speculation, in the case of meniscus injury, MSCs are mobilized from synovium into synovial fluid, and these cells adhere to the injured meniscus. However, the number of MSCs suspended in the synovial fluid and attached to the site is too low to repair or regenerate the injured meniscus, explaining poor spontaneous healing potential of meniscus. Intra-articular injection of synovium-MSCs can boost natural healing ability for meniscal regeneration.

Intravenous infusion of synovium-MSCs may be another route for administration. Although promising results were reported with i.v. infusion of bone marrow-MSCs in animal disease models [35], contrary views are also reported showing that a large fraction of intravenously infused bone marrow-MSCs are trapped in the lung [36]. Cell therapy for meniscal injury has an advantage in that intra-articular injection is possible instead of systemic injection.

The meniscal-deficient knee is a common problem faced by orthopedic surgeons. Although repair of meniscal lesions is possible in selected cases, the poor healing capacity of the tissue often dictates meniscectomy, the most common treatment for meniscal injury. Although meniscectomy provides pain relief and return to function, the loss of meniscal tissue results in long-term dysfunction and secondary osteoarthritis. Currently, there are multiple strategies for addressing this objective, including meniscal allografts, biologic scaffolds for tissue-engineered replacement tissue, and biologic stimuli for meniscal tissue regeneration. In this study, we focused on meniscal regeneration by using synovium-MSCs. Our method has a possibility of regenerating meniscus with less invasion in comparison with meniscal transplantation.

Conclusion

Synovium-MSCs injected into the massive meniscectomized knee adhered to the lesion, differentiated into meniscal cells

directly, and promoted meniscal regeneration without mobilization to distant organs.

ACKNOWLEDGMENTS

We thank Miyoko Ojima for expert help with histology, Yasuko Sakuma for help with animal experiments, and Noriko Hashimoto for skillful technical assistance with microarray and real-time PCR analyses. This study was supported by grants from "the Japan Society for the Promotion of Science (16591478)" to I.S. and "the Japanese Ministry of Education Global Center of Excellence (GCOE) Program, International Research Center for Molecular Science in Tooth and Bone Diseases" to T.M.

DISCLOSURE OF POTENTIAL CONFLICTS OF INTEREST

The authors indicate no potential conflicts of interest.

REFERENCES

1 Wieland HA, Michaelis M, Kirschbaum BJ et al. Osteoarthritis—An untreatable disease? Nat Rev Drug Discov 2005;4:331–344.
2 Chen FH, Rousche KT, Tuan RS. Technology insight: Adult stem cells in cartilage regeneration and tissue engineering. Nat Clin Pract Rheumatol 2006;2:373–382.
3 Ratajczak W. Early development of the cruciate ligaments in staged human embryos. Folia Morphol (Warsz) 2000;59:285–290.
4 Sakaguchi Y, Sekiya I, Yagishita K et al. Comparison of human stem cells derived from various mesenchymal tissues: Superiority of synovium as a cell source. Arthritis Rheum 2005;52:2521–2529.
5 Yoshimura H, Muneta T, Nimura A et al. Comparison of rat mesenchymal stem cells derived from bone marrow, synovium, periosteum, adipose tissue, and muscle. Cell Tissue Res 2007;327:449–462.
6 Morito T, Muneta T, Hara K et al. Synovial fluid-derived mesenchymal stem cells increase after intra-articular ligament injury in humans. Rheumatology (Oxford) 2008;47:1137–1143.
7 Zhang S, Muneta T, Morito T et al. Autologous synovial fluid enhances migration of mesenchymal stem cells from synovium of osteoarthritis patients in tissue culture system. J Orthop Res 2008;26:1413–1418.
8 Hakamata Y, Murakami T, Kobayashi E. "Firefly rats" as an organ/cellular source for long-term in vivo bioluminescent imaging. Transplantation 2006;81:1179–1184.
9 Inoue H, Ohsawa I, Murakami T et al. Development of new inbred transgenic strains of rats with LacZ or GFP. Biochem Biophys Res Commun 2005;329:288–295.
10 Sekiya I, Larson BL, Vuoristo JT et al. Adipogenic differentiation of human adult stem cells from bone marrow stroma (MSCs). J Bone Miner Res 2004;19:256–264.
11 Sekiya I, Vuoristo JT, Larson BL et al. In vitro cartilage formation by human adult stem cells from bone marrow stroma defines the sequence of cellular and molecular events during chondrogenesis. Proc Natl Acad Sci USA 2002;99:4397–4402.
12 Kato A, Homma T, Batchelor J et al. Interferon-α/β receptor-mediated selective induction of a gene cluster by CpG oligodeoxynucleotide 2006. BMC Immunol 2003;4:8.
13 Quackenbush J. Computational analysis of microarray data. Nat Rev Genet 2001;2:418–427.
14 Contag PR, Olomu IN, Stevenson DK et al. Bioluminescent indicators in living mammals. Nat Med 1998;4:245–247.
15 Ichinose S, Tagami M, Muneta T et al. Morphological examination during in vitro cartilage formation by human mesenchymal stem cells. Cell Tissue Res 2005;322:217–226.
16 Murphy JM, Fink DJ, Hunziker EB et al. Stem cell therapy in a caprine model of osteoarthritis. Arthritis Rheum 2003;48:3464–3474.
17 Caplan AI, Dennis JE. Mesenchymal stem cells as trophic mediators. J Cell Biochem 2006;98:1076–1084.
18 Abdel-Hamid M, Hussein MR, Ahmad AF et al. Enhancement of the repair of meniscal wounds in the red-white zone (middle third) by the injection of bone marrow cells in canine animal model. Int J Exp Pathol 2005;86:117–123.
19 Agung M, Ochi M, Yanada S et al. Mobilization of bone marrow-derived mesenchymal stem cells into the injured tissues after intra-articular injection and their contribution to tissue regeneration. Knee Surg Sports Traumatol Arthrosc 2006;14:1307–1314.
20 Ochi M, Uchio Y, Okuda K et al. Expression of cytokines after meniscal rasping to promote meniscal healing. Arthroscopy 2001;17:724–731.
21 Nimura A, Muneta T, Koga H et al. Increased proliferation of human synovial mesenchymal stem cells with autologous human serum: comparisons with bone marrow mesenchymal stem cells and with fetal bovine serum. Arthritis Rheum 2008;58:501–510.
22 Wakitani S, Takaoka K, Hattori T et al. Embryonic stem cells injected into the mouse knee joint form teratomas and subsequently destroy the joint. Rheumatology (Oxford) 2003;42:162–165.
23 Takahashi K, Yamanaka S. Induction of pluripotent stem cells from mouse embryonic and adult fibroblast cultures by defined factors. Cell 2006;126:663–676.
24 Koga H, Shimaya M, Muneta T et al. Local adherent technique for transplanting mesenchymal stem cells as a potential treatment of cartilage defect. Arthritis Res Ther 2008;10:R84.
25 Koga H, Muneta T, Ju YJ et al. Synovial stem cells are regionally specified according to local microenvironments after implantation for cartilage regeneration. Stem Cells 2007;25:689–696.
26 Segawa Y, Muneta T, Makino H et al. Mesenchymal stem cells derived from synovium, meniscus, anterior cruciate ligament, and articular chondrocytes share similar gene expression profiles. J Orthop Res 2008 [Epub ahead of print].
27 Koga H, Muneta T, Nagase T et al. Comparison of mesenchymal tissues-derived stem cells for in vivo chondrogenesis: Suitable conditions for cell therapy of cartilage defects in rabbit. Cell Tissue Res 2008;333:207–215.
28 Mizuno K, Muneta T, Morito T et al. Exogenous synovial stem cells adhere to defect of meniscus and differentiate into cartilage cells. J Med Dent Sci 2008;55:101–111.
29 Cannon WD Jr., Vittori JM. The incidence of healing in arthroscopic meniscal repairs in anterior cruciate ligament-reconstructed knees versus stable knees. Am J Sports Med 1992;20:176–181.
30 Arnoczky SP, Warren RF. The microvasculature of the meniscus and its response to injury. An experimental study in the dog. Am J Sports Med 1983;11:131–141.
31 Bendjaballah MZ, Shirazi-Adl A, Zukor DJ. Biomechanics of the human knee joint in compression: Reconstruction, mesh generation and finite element analysis. Knee 1995;2:69–79.
32 Gabrion A, Aimedieu P, Laya Z et al. Relationship between ultrastructure and biomechanical properties of the knee meniscus. Surg Radiol Anat 2005;27:507–510.
33 McDevitt CA, Webber RJ. The ultrastructure and biochemistry of meniscal cartilage. Clin Orthop Relat Res 1990;8–18.
34 McGonagle D, Jones E. A potential role for synovial fluid mesenchymal stem cells in ligament regeneration. Rheumatology (Oxford) 2008;47:1114–1116.
35 Iso Y, Spees JL, Serrano C et al. Multipotent human stromal cells improve cardiac function after myocardial infarction in mice without long-term engraftment. Biochem Biophys Res Commun 2007;354:700–706.
36 Lee RH, Seo MJ, Pulin AA et al. The CD34-like protein PODXL and {alpha}6-integrin (CD49f) identify early progenitor MSCs with increased clonogenicity and migration to infarcted heart in mice. Blood 2009;113:816–826.

1．高分子
4）糖鎖による軟骨細胞機能制御の可能性
-軟骨変性に伴うN-結合型糖鎖の変化より-

岩崎倫政・松橋智弥・瓜田　淳
高畑雅彦・三浪明男・西村紳一郎

要旨

軟骨組織変性を基本病態とする変形性関節症の発症早期よりN-結合型糖鎖に変化が生じた。この変化は，本疾患の発症病因である軟骨細胞のアポトーシスや細胞外マトリクス分解酵素の分泌に関与していると考えられる。更なる研究により，糖鎖による軟骨細胞の機能制御や関節疾患への関与などが明らかになっていくものと考えられる。これらが明らかになると，糖鎖生物学および糖鎖工学的アプローチによる新たな治療法の開発や，再生医療用マテリアルの開発が可能になるであろう。

キーワード

糖鎖，N-結合型糖鎖，軟骨，軟骨細胞，運動器組織，変形性関節症

はじめに

高齢化社会に突入した現代において，高齢者の運動機能障害は大きな社会問題となっている。運動機能障害をきたす運動器疾患のうち最も頻度の高いものは変形性関節症（osteoarthritis：OA）をはじめとする関節疾患である。2006年のWHOの報告では，日本を含む西側先進諸国におけるOAの発症頻度は65歳以上の全人口の75%に達し，そのうちの85%の患者に何らかの日常生活動作の制限を認めるとしている。さらに，この報告では各国の経済活動に及ぼすOAの影響についても言及しており，労働制限の原因疾患として，OAは循環器系疾患に次ぐものであり，各国のGNPの約1～2.5%の損失原因になるとしている。しかし，その病因については，いまだ十分には解明されてはおらず，決定的な治療法もないのが現状である。OAをはじめとする関節疾患の病因を解明し，その発症および進行を予防する研究を行うことは，医学的見地からのみならず社会・経済的側面からも極めて重要である。

OAをはじめとする多くの関節疾患において治療ターゲットとなる関節軟骨は，血管および神経組織をもたず，少数の軟骨細胞と豊富な細胞外マトリクス（extracellular matrix：ECM）成分により構成される極めてユニークな組織である。したがって，軟骨組織の恒常性維持には，軟骨細胞-ECM間の相互作用（interaction）が極めて重要であると考えられている。この相互作用を理解することが，OAをはじめとする関節疾患の病因を解明することにつながり，さらには軟骨細胞の機能調節機構の解明にも結びつくと予想される。

糖鎖科学はポストゲノム時代の新たな生物科学として，近年その重要性が非常に高まっている。主要な糖鎖遺伝子のクローニングの成果を基盤として，様々な生物学的局面における糖鎖のもつ多彩な機能が明らかになり，疾患との直接的な関連性も証明されてきた[1)2)]。なかでも，細胞表面に局在する糖鎖は「細胞の顔」として，接着，細胞マーカー，シグナル伝達など重要な生理機能を有する。われわれは糖鎖がもつこのような多彩な機能に注目し，軟骨細胞の恒常性維持には糖鎖が重要な役割を果たしているだろうとの仮説のもと，軟骨組織の糖鎖解析と軟骨変性に伴う糖鎖構造の変化を明らかにしてきた。本稿において，その成果を紹介

表❸のような細胞への刺激応答の制御の知見をもとに，前駆細胞，細胞の足場となる多孔質材料，細胞の増殖・分化を促す細胞増殖因子などのシグナル因子をともに移植して体内での組織再構築を図っている。しかしながら，足場材料には細胞との親和性や適切な形状・強度，また正常組織に置換するための生体内分解性など制御すべき多くの性質がある。シグナル因子に関しても，そのままの投与では生体内半減期が短く（数分～数時間），効果が限定的であり，細胞に適切な濃度・時間で作用させるための技術が必要とされている。

これらの問題に対するタンパク質を用いた足場材料やシグナル因子担体の設計は，材料の細胞に対する親和性の高さおよび分解産物の安全性などから多くの検討が行われている。各論は他稿に詳しいが，われわれのグループでも，Ⅰ型コラーゲンスポンジを用いた骨，皮膚，毛，歯周・脂肪組織の再生誘導やスポンジの力学補強による再生効率の向上，ゼラチンハイドロゲルを用いたシグナル因子の徐放とそれによる種々の組織の再生誘導および複数の因子の徐放による効果を報告している[6)-8)]。また，細胞増殖因子の徐放が可能なゼラチンからなるスポンジを作製し，細胞足場とシグナル因子徐放化の両方の機能をもつ ECM に近い次世代足場を開発している[9)]。これらの研究は，タンパク質を用いた足場材料設計は細胞周辺環境として有用であることを示している。加えて，フィブリンを用いた足場材料と細胞増殖因子の複合化や細胞増殖因子を固定したコラーゲンスポンジを用いた血管新生の促進などの報告もある[5) 10) 11)]。

Ⅴ．今後の展望

これまで述べてきたように，タンパク質は遺伝子で蓄積された情報を的確に発現して機能を果たすことで，生体内で重要な役割を担っている。さらに，タンパク質などからなる ECM およびシグナル因子による細胞周辺への構造構築と表面への適切な呈示が細胞の種々の応答に対して大きな役割をもつことも明らかとなっている。また，周囲の環境による細胞応答の制御に関しては，ここ数年のうちにさらに様々な知見が報告されている。Zhang ら[12)]，Calvi ら[13)] は多分化能をもつ幹細胞と呼ばれる細胞が体内に存在し，体内でニッチ（niche）と呼ばれる微小環境にとどまることでその性質を維持していることを報告している。加えて，培養表面に関する細胞応答に関しても，力学強度[14)] や接着面積[15)]，ゲル内での培養による三次元化[16)] などによって，増殖や分化状態が変化することも近年報告されている。このような報告はすべて生体内と同様の環境を細胞に提供した場合に適切な分化挙動が得られるといったものであり，これらの知見を生かして人工 ECM として細胞応答を制御できる材料をいかに作製するかがわれわれに求められている。また今後，更なる生物医学研究の進歩によって，ECM タンパク質，シグナル因子，受容体タンパク質との詳細な相互作用の解明が期待される。それらの知見をもとに新しい人工タンパク質をデザインする，あるいは細胞の周辺環境を構築するといったこともわれわれには必要となってくるであろう。

参考文献

1）井上祥平：生体高分子 - 機能とそのモデル, 化学同人, 1984.
2）関口清俊：再生医療のための細胞生物学, コロナ社, 2007.
3）Petsko G, Ringe D：タンパク質の構造と機能 ゲノム時代のアプローチ, メディカル・サイエンス・インターナショナル, 2005.
4）稲田祐二：タンパク質ハイブリッド（1 ～ 3 巻），共立出版, 1987 - 1990.
5）Lutolf MP, Hubbell JA : Nat Biotechnol 23, 47-55, 2005.
6）Marui A, Kanematsu A, et al : J Vasc Surg 41, 82-90, 2005.
7）Tabata Y : J Drug Target 14, 483-495, 2006.
8）田畑泰彦：臨床外科 62, 1497-1506, 2007.
9）Takahashi Y, Yamamoto M, et al : Biomaterials 26, 4856-4865, 2005.
10）Ito Y : Soft Matter 4, 46-56, 2008.
11）Kong HJ, Mooney DJ : Nat Rev Drug Discov 6, 455-463, 2007.
12）Zhang J, Niu C, et al : Nature 425, 836-841, 2003.
13）Calvi LM, Adams GB, et al : Nature 425, 841-846, 2003.
14）Engler AJ, Sen S, et al : Cell 126, 677-689, 2006.
15）Ingber DE : J Cell Sci 116, 1397-1408, 2003.
16）Gerecht S, Burdick JA, et al : Proc Natl Acad Sci USA 104, 11298-11303, 2007.

木村　祐　プロフィール

2009 年　京都大学大学院工学研究科高分子化学専攻
博士後期課程修了
京都大学先端技術グローバルリーダー養成
プログラム研究員

図❶ 軟骨組織中の N- 結合型糖鎖解析方法

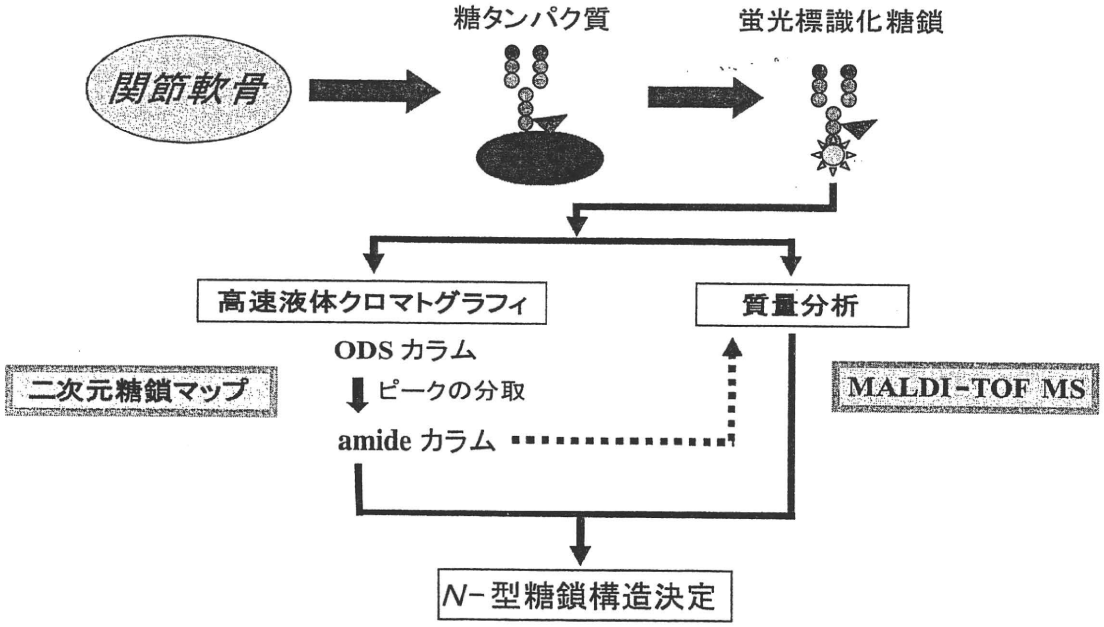

図❷ 軟骨および血清中の糖鎖構造解析結果（文献 8 より）

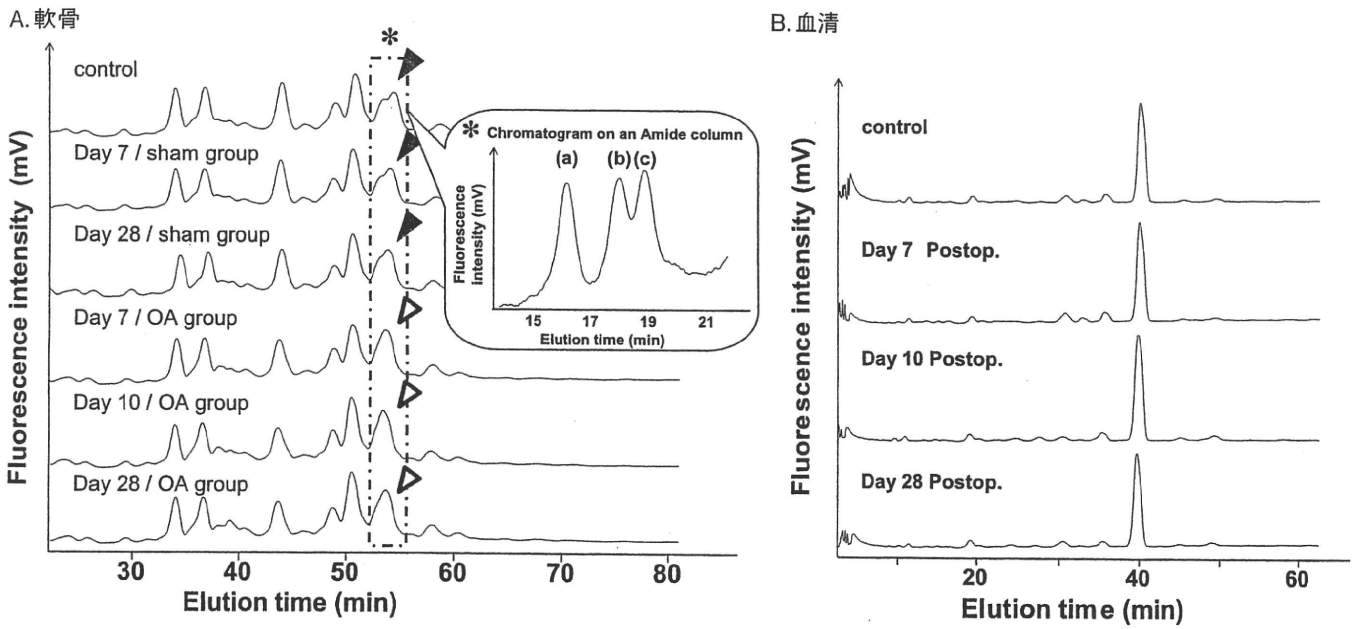

A. 術後 7 日目より OA グループにおいて軟骨中の N- 結合型糖鎖構造の変化を示すピークパターンの変化を認める。
B. 血清中の N- 結合型糖鎖構造には変化を認めない。

Reprinted from Osteoarthritis and Cartilage, Vol.16, Matsuhashi T, Iwasaki N, et al, Alteration of N-glycans related to articular cartilage deterioration after anterior cruciate ligament transection in rabbits, 772-778, Copyright (2008), with permission from Elsevier.

つの複合型 N- 結合型糖鎖が同定された。1 つは 1A1-210.4b（図❸ A）であり，これは OA 軟骨中で発現が増加していた。一方，210.41b（図❸ B）は OA 組織中では発現が減少していた。なお，血清中の N- 結合型糖鎖は正常と OA 軟骨間に有意な変化は認めなかった（図❷ B）。

3. 軟骨組織中の N- 結合型糖鎖の機能

上述したように軟骨組織の OA 変化の極めて早期より N- 結合型糖鎖に変化が生じていることが明らかとなった。一般に OA の発症初期には，その発症誘因となる何らかの刺激に軟骨細胞が反応し，アポトーシスや ECM 分解酵素の分泌が生じるとされている。これらが引き金となり，ECM の分解が促進され，軟骨組織の変性が生じていくとされる[9)-11)]。したがって，今

糖鎖がもつ生体内での軟骨細胞の機能調節について言及したい。

Ⅰ. *N*-結合型糖鎖

糖鎖は，グルコースやガラクトースなどの糖が鎖状に連なった物質で，細胞表面やタンパク質（糖タンパク質），脂質（糖脂質）の先端に結合し存在する。動物が作り出す糖タンパク質は大きく2つに大別される。アスパラギン（N）残基の酸アミドに結合する *N*-結合型糖鎖と，セリンあるいはスレオニン残基の水酸基に結合する *O*-結合型糖鎖である。このうち，*N*-結合型糖鎖は見かけ上著しい多様性があり，主にマンノースとN-アセチルグルコサミンからなる高マンノース型，ガラクトース，シアル酸，フコースが結合した複合型，さらには混成型，哺乳動物にはこれまで見出されていないキシロース含有型のサブグループがある（**表❶**）[3]。われわれは，軟骨組織の糖鎖の中で，この *N*-結合型糖鎖をターゲットにした解析を行ってきた。

1. 軟骨組織中の *N*-結合型糖鎖解析（図❶）

生後15週齢の成熟日本白色家兎の膝正常軟骨組織および前十字靭帯切断により生じさせたOA（変性）軟骨を経時的に採取し，解析を行った。採取した軟骨片をタンパク質消化酵素のトリプシン，キモトリプシン，プロナーゼ，糖鎖遊離酵素のN-グリコシダーゼFにて処理して *N*-結合型糖鎖を切り出す。その切り出した *N*-結合型糖鎖をゲル濾過することにより精製する。精製した *N*-結合型糖鎖を2-アミノピリジンにてピリジルアミノ（PA）化して蛍光標識化し，それをゲル濾過にて精製する[4][5]。そして，精製した蛍光標識化糖鎖を二次元高速液体クロマトグラフィ（HPLC）法にて解析する[6]。具体的にはODSカラムにて疎水性分画して変化のあった糖鎖を分取し，それをamideカラムにて親水性分画する。それぞれの分析で得られた溶出時間をグルコース・ユニット値に変換し，データベース検索により候補となる糖鎖を絞り込む。最終的には，分取した糖鎖の質量分析による解析などを行うことにより糖鎖を同定する[7]。

2. OA変化に伴う軟骨組織中の糖鎖変化[8]

OA軟骨においては，明らかな組織学的変化が生じる以前の術後7日目より *N*-結合型糖鎖構造の変化を示すピークパターンの変化が認められた（**図❷A**）。この変化をさらに解析することにより，変化している2

表❶　*N*-結合型糖鎖のサブグループと構造（文献3より）

サブグループ	糖鎖構造
複合型	Galβ1-4GlcNAcβ1 ⟍ 6 Galβ1-4GlcNAcβ1 — 4 Manα1 Galβ1-4GlcNAcβ1 ⟋ 2 Galβ1-4GlcNAcβ1 ⟍ 4 Manα1 Galβ1-4GlcNAcβ1 ⟋ 2 GlcNAcβ1 — 4 — Manβ1-4GlcNAcβ1-4GlcNAc -Asn Fucα1 — 6
高マンノース型	Manα1-2 Manα1 ⟍ 6 Manα1-2 Manα1 ⟋ 3 Manα1 Manα1-2 Manα1 — 2 Manα1 Manβ1-4GlcNAcβ1-4GlcNAc -Asn
混成型	Manα1 ⟍ 6 Manα1 ⟋ 3 Manα1 GlcNAcβ1 ⟍ 4 Galβ1-4GlcNAcβ1 ⟋ 2 Manα1 Manβ1-4GlcNAcβ1-4GlcNAc -Asn 4 — GlcNAcβ1 6 — Fucα1
キシロース含有型	Manα1 ⟍ 6 Manα1 ⟋ 3 Manα1 Manβ1-4GlcNAcβ1-4GlcNAc -Asn 2 — Xylβ1 3 — Fucα1

出典　糖と脂質の生物学（シリーズ・バイオサイエンスの新世紀 第4巻），1-7, 2001, 共立出版より許可を得て転載

図❸　軟骨中で変化していた複合型 *N*- 結合型糖鎖（文献 8 より）

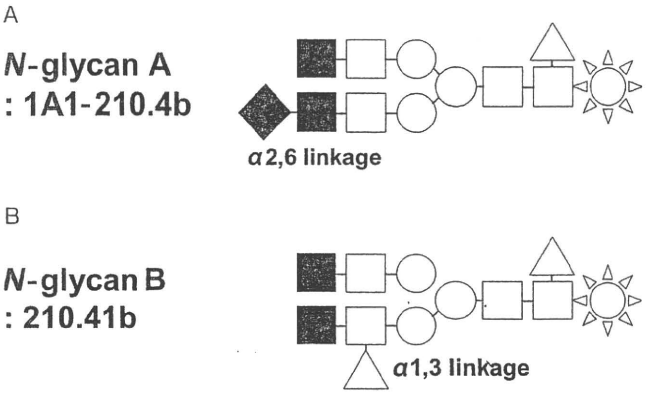

A. OA 軟骨中で発現が増加していた 1A1-210.4b
B. OA 組織中では発現が減少していた 210.41b

Reprinted from Osteoarthritis and Cartilage, Vol.16, Matsuhashi T, Iwasaki N, et al, Alteration of *N*-glycans related to articular cartilage deterioration after anterior cruciate ligament transection in rabbits, 772-778, Copyright (2008), with permission from Elsevier.

回同定した *N*- 結合型糖鎖は，OA 変化を生じさせる軟骨細胞の機能調節に関与していると推測される。現在，レクチン染色による *N*- 結合型糖鎖の局在，軟骨細胞中の関連する糖鎖関連酵素遺伝子のノックダウンにより同定した糖鎖の機能解析を進めている。

Ⅱ．糖鎖による運動器組織細胞の機能制御

われわれはウサギ軟骨 OA（変性）モデルを用いて，軟骨中の糖鎖が発症の極めて早期より変化し，軟骨細胞のアポトーシスや ECM 分解酵素の分泌を促進している可能性を示した。誌面の都合上，詳細は記載しないが，マウス軟骨変性モデルを用いて，軟骨変性に伴い軟骨細胞のある種の糖鎖関連酵素遺伝子の発現が変化し，それに関連する *N*- 結合型糖鎖にも変化が生じたことを明らかにした。さらに，われわれは同じ運動器組織細胞である破骨細胞に対するシアリル糖鎖の機能解析も行ってきた[12]。

シアル酸は糖鎖先端に存在するアミノ糖の一種であり，様々な細胞表面に糖タンパクや糖脂質の一部として存在する。シアル酸はその構造的多様性や結合様式によって細胞間認識や細胞接着などに関与すると考えられており，ウイルスと細胞の融合や受精，赤血球の貪食などにおいても重要な役割を果たすことが報告されている。われわれは，このシアル酸を含むシアリル糖鎖が骨の新陳代謝に関与する破骨細胞にも豊富に発現しており，その分化制御機構に関わる可能性があることを明らかにしてきた。血球系幹細胞を起源とするマクロファージ系細胞である破骨前駆細胞には，ガラクトースと α (2,3) 結合または α (2,6) 結合するシアル酸がともに発現しており，これらは RANKL 刺激後に発現が増加し，細胞膜へ集積する傾向がみられた。さらに，分化の最終段階である細胞融合した多核成熟破骨細胞では，α (2,6) 結合シアル酸の発現が減少することがわかった。この細胞表面に発現するシアル酸を外因性シアリダーゼで除去すると破骨前駆細胞は TRAP 陽性単核細胞までは分化したが，多核巨細胞を形成できないことがわかった（図❹）。また，シアル酸転移酵素の 1 つである β galactoside α (2,6) sialyltransferase-I

図❹　骨髄マクロファージから M-CSF と RANKL を用いた破骨細胞分化系における細胞表面糖鎖除去による影響（文献 12 より）

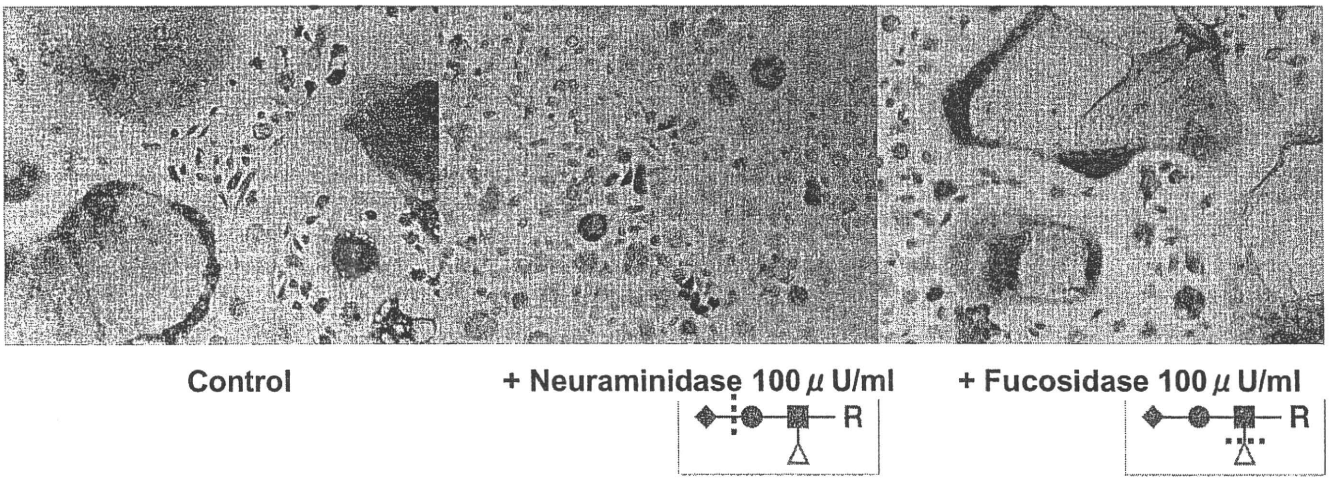

コントロールやフコシダーゼ（フコース切断酵素）で処理した細胞では，酒石酸抵抗性酸ホスファターゼ陽性の多核巨細胞（成熟破骨細胞）が形成されているが，ノイラミニダーゼ（シアル酸切断酵素）で処理した細胞は，多核巨細胞の形成が阻害されている。（× 200 倍）

Reprinted from Bone, Vol.41, Takahata M, Iwasaki N, et al, Sialylation of cell surface glycoconjugates is essential for osteoclastogenesis, 77-86, Copyright (2007), with permission from Elsevier.

（ST6Gal-I）遺伝子の発現をノックダウンした細胞でも同様に多核破骨細胞の形成が阻害されたことから，シアリル糖鎖が破骨細胞の分化，特に細胞融合過程において重要な役割を果たしている可能性が示唆された。

このように，糖鎖は生体内において軟骨や骨などの運動器組織細胞の機能制御を担っている可能性があり，運動器疾患の発症にも大いに関与していることが予想される。

❖ おわりに

今後は，軟骨細胞レベルでの N- 結合型糖鎖解析およびその機能の解明を進め，最終的には糖鎖関連酵素遺伝子の組織特異的遺伝子破壊動物を作製し，生体内での軟骨組織に対する糖鎖機能の解明を行っていく予定である。糖鎖生物学的アプローチを用いた OA の病因解明に関する研究は，これまでほとんど行われていない。OA 研究に糖鎖生物学を融合させることにより，今まで明らかにされなかった新たな知見が得られ，予防法や治療法の開発につながっていくと考えられる。さらに，糖鎖を基盤マテリアルに導入することにより，軟骨細胞の接着性や増殖性の制御が可能な機能性 scaffold マテリアルが開発され，軟骨再生医療への応用も可能になると考える。

参考文献

1）Wang X, Inoue S, et al : Proc Natl Acad Sci USA 102, 15791-15796, 2005.
2）Yamashita K, Ideo H, et al : J Biol Chem 268, 5783-5789, 1993.
3）木幡　陽：糖と脂質の生物学（シリーズ・バイオサイエンスの新世紀第 4 巻），1-7, 共立出版, 2001.
4）Hase S, Ikenaka T, et al : Biochem Biophys Res Commun 85, 257-263, 1978.
5）Nakagawa H, Kawamura Y, et al : Anal Biochem 226, 130-138, 1995.
6）Tomiya N, Awaya J, et al : Anal Biochem 171, 73-90, 1988.
7）Kurogochi M, Nishimura S-I : Anal Chem 76, 6097-6101, 2004.
8）Matsuhashi T, Iwasaki N, et al : Osteoarthritis Cartilage 16, 772-778, 2008.
9）Bluteau G, Conrozier T, et al : Biochim Biophys Acta 1526, 147-158, 2001.
10）Goldring MB : Arthritis Rheum 43, 1916-1926, 2000.
11）Malfait AM, Liu RQ, et al : J Biol Chem 277, 22201-22208, 2002.
12）Takahata M, Iwasaki N, et al : Bone 41, 77-86, 2007.

岩崎倫政　プロフィール

1998 年　北海道大学大学院医学研究科外科系専攻博士課程修了
2000 年　同運動器再建医学分野助手
2005 年　北海道大学医学部附属病院整形外科講師

The Use of Laser Capture Microdissection on Adult Human Articular Cartilage for Gene Expression Analysis

Naoshi Fukui, Yasuko Ikeda, and Nobuho Tanaka

Abstract

The integrity of articular cartilage is maintained by chondrocytes, the sole type of cell that resides within the tissue. The non-calcified region of articular cartilage can be divided into three zones based on histological features, in which the chondrocyte metabolism is known to differ obviously among the zones. In pathological cartilage, the chondrocyte metabolism may change dramatically, which could play a pivotal role in the progression of the disease. Since such change in metabolism differs obviously from site to site within cartilage, it is crucial to determine the chondrocyte metabolism in respective regions. To this end, we have employed laser capture microdissection (LCM) to analyze chondrocyte metabolism in various regions of pathological and control cartilage. In this report, we describe our protocol for LCM on adult human cartilage tissue. With this protocol, a specific site of cartilage tissue was successfully obtained by LCM for gene expression analysis.

Key Words: Laser capture microdissection; articular cartilage; mRNA; osteoarthritis; chondrocyte; metabolic change; regional difference.

1. Introduction

Articular cartilage is a thin layer of connective tissue which covers bone surfaces within synovial joints. It is a unique tissue for the capacity to withstand repetitive loads, allowing frictionless motion of the joint. Articular cartilage is primarily composed of water and extracellular matrix, with a small volume of cells. The matrix of articular cartilage is composed of several types of collagen and proteoglycans (*1*). Chondrocytes are the only kind of cell that resides within cartilage, and since no other types of cells are seen in cartilage, chondrocytes are considered to be entirely responsible for the integrity and turnover of cartilage matrix.

Based on histological features, articular cartilage can be divided into four layers of superficial (tangential), middle (transitional), deep (radial) zones and calcified cartilage underneath (*1-3*) (Figure 1). Among them, calcified cartilage is unique in that the matrix contains an abundance of calcium apatite crystals and is clearly distinguished from the above three zones by a tide mark. In the three non-calcified zones, the metabolic activity of chondrocytes is known to differ considerably among the zones (*1, 2, 4-6*).

Osteoarthritis (OA) is a disease that primarily affects articular cartilage. In OA, the cartilage matrix is lost gradually over years, eventually devastating functional joints. OA is an age-related disease. With the aging of society, OA has become the most prevalent joint disease in developed countries (*7*). OA of a knee joint is particularly an issue, in view of its prevalence, severity of symptoms, and association with disability (*8, 9*).

Focal loss of articular cartilage is a unique feature in the pathology in OA. In OA joints, cartilage is most severely degenerated in weight-bearing areas, but may remain almost intact in non-weight-bearing areas. Reflecting such regional differences, the chondrocyte metabolism differs considerably from site to site within cartilage. Since chondrocytes become catabolic and promote cartilage degeneration in OA, it is critically important to determine chondrocyte metabolism at respective sites within OA cartilage. Conventionally, such regional differences can be known only by histological methods, such as immunohistochemistry or in situ hybridization.

Laser capture microdissection (LCM) is an innovative technology that enables acquisition of specific sites of the tissues based on histological features. We have employed this method and successfully analyzed gene expression levels of chondrocytes in respective regions of OA and control cartilage. In this section, we describe in detail our LCM protocol for adult human articular cartilage tissue. The use of LCM on cartilage

tissue could clarify many novel aspects of cartilage pathology, which cannot be known by any other methods.

2. Materials and Labware

2.1 Preparation of Cartilage Tissue Blocks

1. DMEM/F-12 (Life Technologies, Carlsbad, CA).
2. Scalpel blade (No. 15; Feather, Osaka, Japan).
3. Scalpel holder (No. 3; Feather).
4. Optimum Cutting Temperature (OCT) compound (Sakura Finetek Japan, Tokyo, Japan).
5. Metal mold for tissue blocks.
6. Liquid nitrogen.
7. Deep freezer (-80°C).

2.2 Sectioning

1. Cryostat (CM1900; Leica Microsystems, Houston, TX).
2. Disposable microtome blades (818; Leica Microsystems).
3. Precleaned glass slide (S2444; Matsunami, Osaka, Japan).
4. RNAse-free water (Nippon Gene, Tokyo, Japan).
5. Ethylenediaminetetraacetic acid disodium salt (EDTA) solution, 0.5M (E7889; Sigma, St. Louis, MO).
6. Ethanol (054-07225; Wako Pure Chemical, Osaka, Japan).
7. Xylene (320579; Sigma).
8. RNase-free pipet tips and pipettes (1000, 200, 20 μl).
9. Lint-free paper towels.
10. Fume hood.

2.3 LCM

1. Laser Capture Microdissection System (Arcturus PixCell IIe; Molecular Devices, Sunnyvale, CA).
2. LCM caps (CapSure LCM caps; Molecular Devices).
3. Fine-pointed tweezers.
4. (Optional) Dissection microscope.

2.4 RNA Extraction

1. RNeasy Micro kit (74004; Qiagen, Hilden, Germany).
2. 2-mercaptoethanol (M7154; Sigma).

3. Ribosomal RNA from E. coli (206938; Roche Diagnostics, Bazel, Switzerland). Dissolve in RNase-free water at a concentration of 10 μM.
4. Tabletop centrifuge.
5. Clean, autoclaved 1.5 ml centrifuge tubes.

2.5 cDNA Synthesis

6. Sensiscript RT kit (205211; Qiagen).
7. Oligo dT primer (18418-020; Life Technologies).
8. RNAse inhibitor (3335399; Roche Diagnostics).
9. Heat block for 1.5 ml centrifuge tubes (37°C).

3. Methods

Due to the ubiquitous presence of RNases, RNA is extremely unstable. To minimize RNA degradation, all reagents and instruments used for the experiment should be RNase-free. Disposable experimental gloves should be worn throughout the procedure, and the experiment should be performed as quickly as possible (*see* **Note 1**).

3.1 Preparation of Cartilage Tissues

1. Cartilage tissue obtained at surgery or dissection is transferred to the laboratory without delay in chilled DMEM/F-12 medium (*see* **Note 2**).
2. Cartilage tissue should be processed immediately after arrival to minimize RNA degradation.
3. Cartilage tissues are separated from the subchondral bone in full thickness with a sharp scalpel (**Fig. 2, A** and **B**). We prefer to use a small crescent-shaped blade to do this.
4. The cartilage tissue is cut into an appropriate size (**Fig. 2, C** and **D**).
5. OCT compound is poured in a mold, and the tissue is placed within it with the cross section of the tissue parallel to the surface (*see* **Notes 3** and **4**). The mold is immediately dipped in liquid nitrogen to solidify the compound (**Fig. 2E**).
6. Remove the compound block from the mold (**Fig. 2F**), put it in an appropriate container, and store it at -80°C until use. In this condition, RNA in the tissue can be preserved for at least 3 years, as long as it is maintained strictly at -80°C.

3.2 Preparation of Cryosections

1. Cryostat is prepared for sectioning. Set a new microtome blade and cool down the chamber and specimen disc holder. We usually set the temperatures of the chamber and the holder at -20°C and -30°C, respectively, but the optimum temperature may differ among cartilage tissues, and may need further optimization. A lower temperature may be better for control cartilage.
2. A tissue block is mounted on a specimen disc and attached to the cryostat. Adjust the orientation of the specimen discs so that the sections will be cut parallel to the cross section of the cartilage tissue (**Fig. 3A**).
3. After waiting for 5-10 min to equilibrate the block temperature, cut cryosections into 20-30 μm thicknesses and mount on a glass slide (*see* **Note 5**). Place three to five sections on one slide in view of possible loss during processing.

4. These sections are immediately processed for LCM (*see* **Note 6**).

3.3 Processing of Tissue Sections for LCM

1. To complete the processing and LCM as quickly as possible, we usually treat one glass slide at a time (*see* **Note 7**).
2. The sections on the glass slide are washed twice briefly with 1-2 ml of ice-cold RNAse-free water to remove the OCT compound. RNAse-free water is placed on a glass slide with a pipette until the entire sections are covered. The water is pipetted up and down several times, and then removed by a pipette.
3. Treat sections with 1-2 ml of 0.5M EDTA solution for 3 min at room temperature.
4. After removing the EDTA solution, sections are rinsed once briefly with ice-cold RNAse-free water (*see* **Note 8**).
5. Sections are then treated with 75%, 95%, and 100% ethanol sequentially, each for 30 sec.
6. Treat with 100% ethanol again for 30 sec (*see* **Note 9**).
7. Finally, treat sections with xylene for 5 min. Then remove xylene with a pipette and a paper towel, and allow the sections to dry up in a fume hood. When completely dry, proceed to LCM immediately (**Fig. 3B**).

3.4 Acquisition of Cartilage Tissues by LCM

1. Place a glass slide and cryosections on the stage of an LCM device (*see* **Note 10**).
2. Identify cartilage zones through the LCM device. We usually use a 2X or 4X objective for this purpose (*see* **Note 11**).
3. The slide is fitted to the stage by a vacuum chuck equipped in the device.
4. Place an LCM cap on the section following the manufacturer's instruction.
5. Alternatively, the cap may be placed manually on the section before setting the glass slide on the stage (**Fig. 3C**).
6. Confirm that the area of interest is seen through the cap (**Fig. 3D**).
7. Pulse the laser in the area outside the section as a trial to adjust the focus. We prefer to set the spot size of the laser at 15 or 30 μm in diameter.
8. The power and duration of the laser are set at 60-100 mW and 1-3 msec, respectively. Since we use thicker sections, these parameters are greater than those for regular LCM.
9. Pulse the laser repeatedly until the area of interest is entirely attached to the plastic film